










Metabolite profiling reveals the influence of grapevine genetic distance on the chemical signature of juices

Hector Alonzo Gomez Gomez,^{a,b}  Guilherme Francio Niederauer,^b 
Igor Otavio Minatel,^c  Elisa Ribeiro Miranda Antunes,^d 
Mara Junqueira Carneiro,^b 
Alexandra Christine Helena Frankland Sawaya,^e  Mauro Celso Zanus,^f
Patrícia Silva Ritschel,^f  Giuseppina Pace Pereira Lima^c  and
Marcia Ortiz Mayo Marques^{b*} 



Abstract

BACKGROUND: Yield, disease tolerance, and climate adaptation are important traits in grapevine genetic breeding programs. Selection for these characteristics causes unpredictable changes in primary and specialized metabolism, affecting the physico-chemical properties and chemical composition of the berries and their processed products, juice, and wine. In this study, we investigated the influence of the genetic distance between grapevine genotypes on the chemical signatures of the juices, by integrating comprehensive metabolic profiling to genetic analyses.

RESULTS: The studied grapevine cultivars exhibited low genetic diversity. Breeding for agronomic traits promoted higher contents of soluble sugars, total phenolics, and anthocyanins in the juices. Untargeted juice metabolomics identified a total of 147 metabolites, consisting of 30 volatiles, 21 phenolics, and 96 ultra-high-performance liquid chromatography–mass spectrometry (UHPLC-MS) features. Juices from grapes of the most recent cultivars exhibited increased levels of *trans*-resveratrol, catechin, and luteolin. The blend of volatiles from juices of later cultivars was also more complex, consisting of 29 distinct metabolites in 'BRS Magna'. Grapes from 'BRS Carmem', an intermediate cultivar, gave the most divergent UHPLC-MS juice profile.

CONCLUSION: Contents of soluble solids, total phenolics, and anthocyanins in grape juices were increased by controlled crosses and hybrid selection. Integrative analyses demonstrated that the juices' metabolic profiles accurately represent the cultivars' genetic distances. Juices from 'BRS Violeta' and 'BRS Magna' show relevant positive association with health-related phenolics and a distinct set of odor volatiles, although these characteristics were specifically sought by breeding.

© 2023 Society of Chemical Industry.

Supporting information may be found in the online version of this article.

Keywords: GC-MS; genetic breeding; grapevine; phenolics; UHPLC; volatiles

INTRODUCTION

Grapes are cultivated worldwide, occupying an area of 6.73 million ha in 2020, from temperate to tropical areas,¹ mainly based on *Vitis vinifera* and *Vitis labrusca* genotypes.² Genetic breeding is considered the main contributor to grapevine adaptation in the face of distinct biotic and abiotic conditions.^{2,3} Most of the traits sought after by grapevine breeding programs are related to the plant's agronomical performance, such as production, drought and temperature tolerance, and disease resistance.²⁻⁴ These traits are complex and depend on the orchestrated function of many developmental, physiological, and metabolic processes that are controlled by large portions of the grapevine genome.^{2,5,6} Therefore, breeding strategies aimed at grapevine agronomical traits may lead to unpredictable changes in the quality of the berry

* Correspondence to: MOM Marques, Plant Genetic Resources Center, Agronomic Institute (IAC), Campinas, São Paulo, 13075-630, Brazil. E-mail: marcia.marques@sp.gov.br

a School of Agriculture, São Paulo State University (UNESP), São Paulo, Brazil

b Plant Genetic Resources Center, Agronomic Institute (IAC), São Paulo, Brazil

c Institute of Biosciences, São Paulo State University (UNESP), São Paulo, Brazil

d Biology Institute, State University of Campinas (UNICAMP), São Paulo, Brazil

e Faculty of Pharmaceutical Sciences, State University of Campinas (UNICAMP), São Paulo, Brazil

f Embrapa, Embrapa Uva e Vinho, Bento Gonçalves, 95701-008, RS, Brazil

and/or its processed products, juice, and wine.² Moreover, the genetic architecture of grape chemical features, mostly investigated in *V. vinifera*, has been demonstrated to be inconsistent among different species of the genus, with only a few transferable genetic markers.^{7,8} The complexity of the genetic inheritance of berry chemical traits is probably derived from the intrinsic associations between the primary and specialized metabolism.⁹

Grape juices are natural, non-fermented beverages that retain the typical color, aroma, and flavor of the berries. These features are determined by the contents of products from the primary and specialized metabolism of the grape berries at maturity,⁸⁻¹⁰ and thus ultimately determined by the cultivar's genomic context. In Europe, grape juices are made from berries of winemaking *V. vinifera* cultivars,⁴ whereas in North and South America juices are mainly made from grapes of *V. labrusca* or *V. vinifera* × *V. labrusca* interspecific hybrids. The leading cultivars used by the American juice industry are 'Isabella', 'Bordo/lves', and 'Concord', because of their high productivity, resistance to diseases, nutritional properties, and unique flavors.¹¹ However, these genotypes exhibit uneven maturation, weak coloration, low content of soluble solids, and poor adaptation to warmer climates.⁴

The grapevine breeding program at Embrapa has been continually developing adapted cultivars by clonal selection and controlled crosses.⁴ Cultivars 'Concord Clone 30' and 'Isabel Precoce' were identified from spontaneous somatic mutations of the traditional cultivars 'Concord' and 'Isabella', respectively (Supporting Information, Fig. S1), selected for their advanced phenological cycles, while retaining production and adaptation characteristics of the original cultivars.⁴ Controlled hybridizations were used to develop the cultivar 'BRS Rúbea', which was used as a parent in the subsequent hybridizations originating 'BRS Cora', 'BRS Carmem', 'BRS Violeta', and 'BRS Magna'² (Fig. 1(A–E), Fig. S1). The hybrid genotypes were selected based on climate adaptation, fruitfulness, soluble solids contents, and color,⁴ along three generations of breeding, spanning more than 40 years. Controlled crosses increased the content of proanthocyanidins in the grapes, wines, and seeds of five selections from two progenies of 'Monastrell'.¹² Similarly, berries from a morphological mutant of 'Glera', an important Prosecco wine cultivar, displayed distinct monoterpene and polyphenol profiles, although clones, selected for agronomical performance, had a similar chemical profile to the original genotype.¹³ These studies were restricted to certain metabolic groups, and the genetic distances between the genotypes were not accessed. Thus, to date, studies comparing the genetic and chemical diversity in grapevine remain scarce. The current work was designed to investigate the effect of genetic distance on the metabolic composition of grape juices, from two mutant genotypes and five cultivars obtained by controlled crosses, related by parentage.

MATERIAL AND METHODS

Plant material and genotyping

Grapevines were grown in experimental vineyards in Bento Gonçalves (29.1650° S, 51.5264° W), Brazil, using Paulsen 1103 rootstocks, at 2.5 × 1.5 m spacing, on E–W orientation on a slope of <5%. The plants were trained on a pergola system and subjected to standard phytosanitary and soil management practices. Physicochemical data represent average values from three independent technical juice sample replicates for each cultivar, from five successive vintages (2015–2020). Metabolic

profiles represent data from three technical replicates of juices from the eight genotypes, produced in a representative vintage.

The genotypes consisted of conventional juice cultivars Bordo/lves, Isabel Precoce and Concord Clone 30, somatic mutations of 'Isabella' and 'Concord', respectively, and novel genotypes developed by controlled crossings at Embrapa: 'BRS Rúbea', 'BRS Cora', 'BRS Carmen', 'BRS Violeta', and 'BRS Magna' (Fig. 1). The genotypes' pedigree is shown in Supporting Information, Fig. S1. The plants were genotyped using a set of 14 simple sequence repeat (SSR) molecular markers (Supporting Information, Table S1), including the minimal set recommended for grapevine cultivar analyses.¹⁴ Genomic DNA was isolated from young leaf material, quantified, and submitted to SSR loci amplification by polymerase chain reaction (PCR), as described previously.¹⁵ PCR products were resolved on sequencing gels and fragment lengths were determined by comparison with internal size standards.¹⁰ Genotypic data were analyzed using the adegenet package¹⁶ in R v. 4.2.0.¹⁷ to calculate descriptive genetic parameters, including number of alleles per locus, allelic frequency, observed and expected heterozygosity, and *F*-statistics, along with the polymorphism information content and identity probability for the investigated SSR set and group of cultivars. Pairwise genetic distances were calculated using Bruvo's coefficient to generate agglomerative hierarchical clusters by applying the unweighted pair-group method with arithmetic averages (UPGMA) and multivariate analyses, using adegenet.¹⁶

Berry processing

Juices were processed at the Microvinification Laboratory at Embrapa Grape and Wine, using a modified tube-in-tube method.¹⁸ Briefly, 200 kg hand-picked, selected grapes at physiological maturity, determined by refractometry, from the 2015/2016 growing season, were destemmed, and heated in tanks at 65–80°C for 2 h without removing the skins. After separation of the must from the solid phase, the mixture was transferred to a cold tank for precipitation for 24 h. Subsequently, the liquid was moved to a second tank, heated at 60 °C, pasteurized in the thermal exchange tube (tube-in-tube up to 85 °C), and bottled. Physicochemical analyses were performed for juices from five successive vintages (2015–2019), as three technical replicates, from independent bottles.

Physicochemical and color parameter analyses

Juice quality was analyzed for the following physicochemical parameters: soluble solids content (SSC, Brix), determined using a digital refractometer (RX5000, Atago Co. Ltd, Tokyo, Japan); and titratable acidity (TA) and total phenolics (TPI), by sodium hydroxide titration and Folin–Ciocalteu assay, respectively, as described by the International Organization of Vine and Wine (OIV).¹⁹ Juice color was investigated according to the following CIELAB parameters: lightness (L^*), red–green (a^*), yellow–blue (b^*), chroma (C^*), and tonality angle or hue (h^*), at wavelengths of 450, 520, 570, and 630 nm, using a colorimeter (CR-400, Minolta, Tokyo, Japan), as described previously.²⁰ The values for lightness (L^*) range from 0 (black) to 100 (white), whereas chroma (C^*) indicates the distance from achromatic to a pure chromatic color, calculated from the values of a^* and b^* values from the CIELAB scale system, which begins at zero for completely neutral colors, rising in magnitude with increasing intensity.

Total monomeric anthocyanins

Content of total monomeric anthocyanins was determined by the differential pH method,²¹ using potassium chloride (pH 1.0) and sodium acetate (pH 4.5) buffer solutions. Absorbance

was read at wavelengths of 510 and 700 nm in a spectrophotometer (Ultraspec-2000, Amersham-Pharmacia Biotech, Amersham, UK). Anthocyanin content is presented as mg L⁻¹ malvidin-3,5-diglucoside.

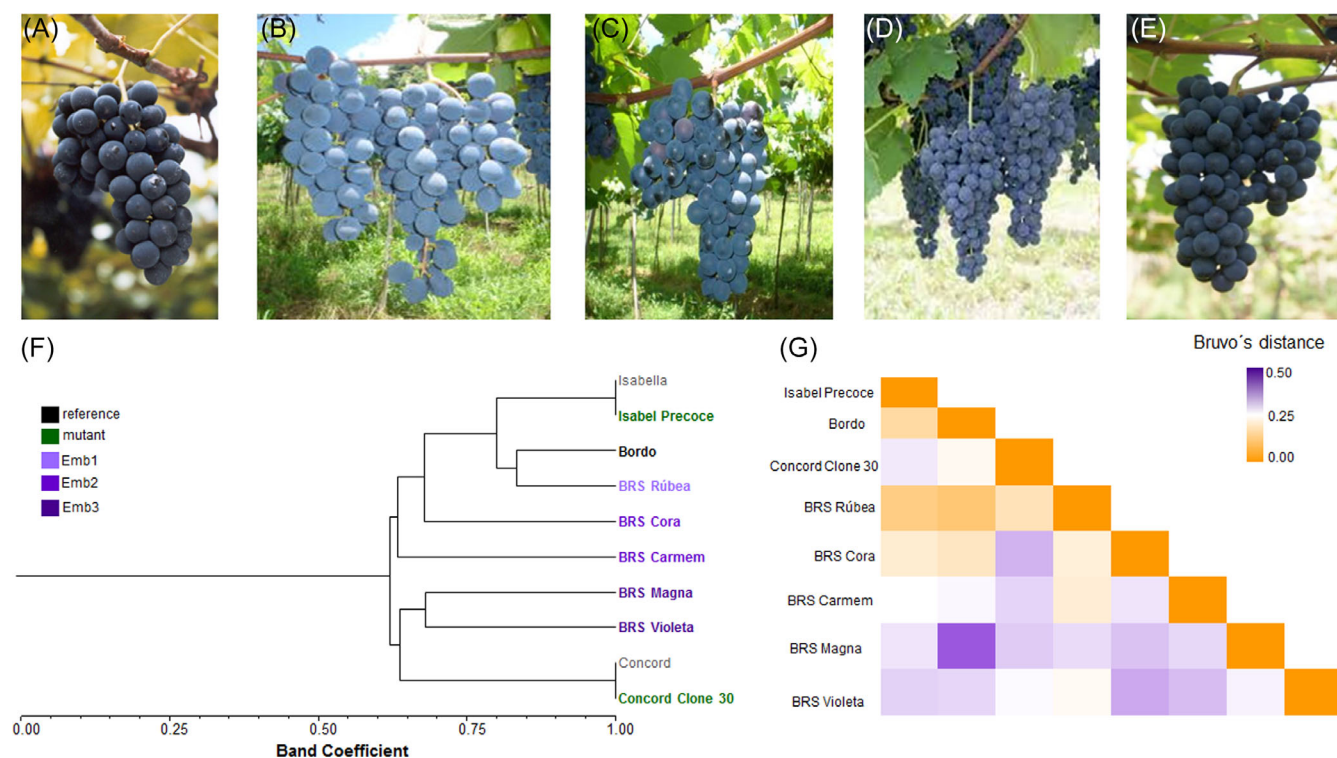


Figure 1. Phenotypic and genetic characterization of Embrapa grapevine juice cultivars. Clusters from BRS Rúbea (A), BRS Cora (B), BRS Carmem (C), BRS Violeta (D), and BRS Magna (E) in standard vineyards. Unweighted pair group method with arithmetic mean (UPGMA) dendrogram (F) and heatmap of the genetic distances (G) between the investigated grapevine cultivars based on a set of 14 simple sequence repeat (SSR) markers.

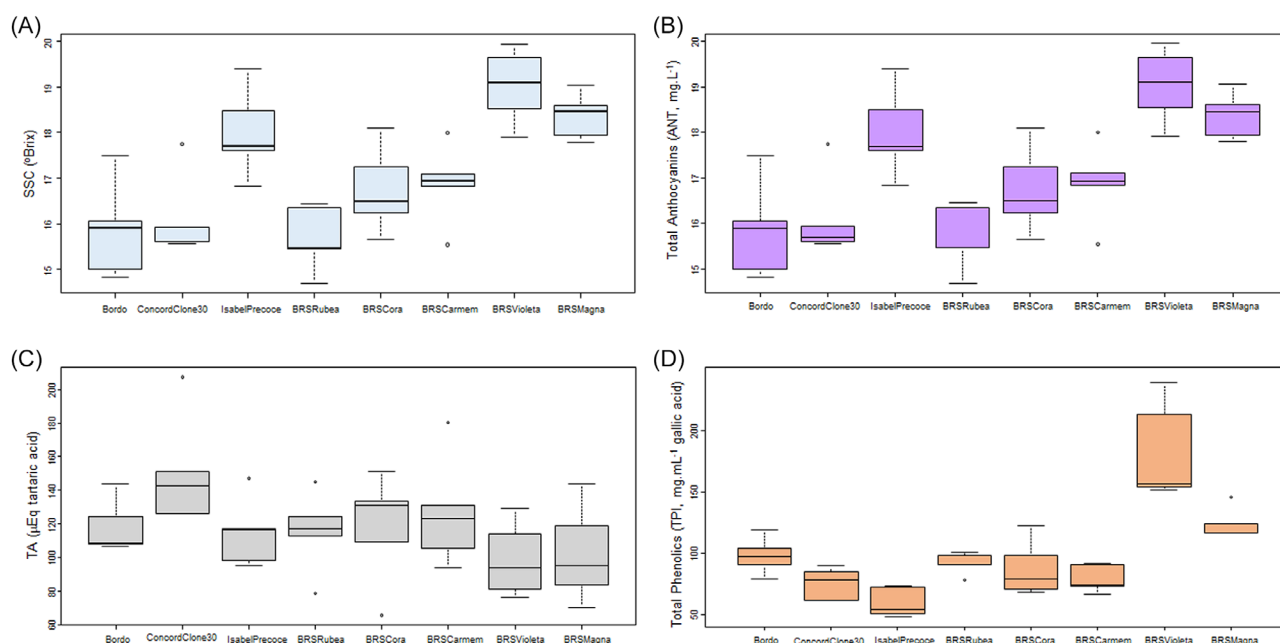


Figure 2. Physicochemical properties of the juices. Soluble solids contents (SSC) (A), total anthocyanins (B), total titratable acidity (TA) (C), and total phenolics (D). Boxplots represent values from triplicate juice samples from five vintages (2015–2019) for each cultivar ($n = 120$); whiskers represent the distances between the maximum or minimum values to the higher and lower quartiles; outliers are shown as dots.

Table 1. Profile of phenolic compounds from grape juices determined by UHPLC analyses. Contents are expressed in mg L⁻¹ and represent means from three replicates per genotype ± standard deviation (*n* = 24)

Metabolite	Molecular formula	RT (min)	Bordo	Isabel Precoce	Concord Cl 30	BRS Rúbea	BRS Cora	BRS Carmen	BRS Violeta	BRS Magna
Anthocyanins										
Cyanidin-3,5-diglucoside	C ₂₇ H ₃₁ O ₁₆	7.13	43.47 ± 2.85d	—	46.16 ± 7.50d	69.22 ± 1.89c	107.28 ± 5.83b	35.55 ± 0.64d	239.56 ± 9.90a	76.62 ± 5.56c
Delphinidin-3-O-glucoside	C ₂₁ H ₂₁ O ₁₂	7.41	29.09 ± 1.22d	25.42 ± 0.09ed	35.10 ± 0.75c	26.71 ± 0.59de	51.76 ± 2.15a	22.77 ± 0.08d	45.62 ± 2.09b	29.02 ± 0.28d
Cyanidin-3-O-glucoside	C ₂₁ H ₂₁ O ₁₁	8.42	2.40 ± 0.41b	1.09 ± 0.06b	8.70 ± 2.45a	—	2.25 ± 0.34b	0.58 ± 0.17b	—	—
Pelargonidin-3-O-glucoside	C ₂₁ H ₂₁ O ₁₀	9.49	—	—	0.43 ± 0.08a	—	0.33 ± 0.04b	—	—	—
Malvidin-3,5-diglucoside	C ₂₉ H ₃₅ O ₁₇	9.64	139.96 ± 29.98ab	9.85 ± 0.63c	5.85 ± 1.81c	107.92 ± 4.25b	2.33 ± 0.22c	116.08 ± 1.14b	129.21 ± 8.35ab	162.10 ± 18.94a
Peonidin-3-O-glucoside	C ₂₂ H ₂₃ O ₁₁	10.86	0.98 ± 0.10b	2.25 ± 0.15a	0.35 ± 0.06de	0.59 ± 0.12cd	0.76 ± 0.09bc	0.21 ± 0.12e	0.89 ± 0.23bc	1.03 ± 0.09b
Malvidin-3-O-glucoside	C ₂₃ H ₂₅ O ₁₂	12.18	6.64 ± 0.48b	9.95 ± 0.43a	3.58 ± 0.04cd	4.08 ± 0.08cd	3.46 ± 0.01d	4.21 ± 0.27c	3.60 ± 0.04cd	3.95 ± 0.10cd
Flavonols										
Rutin	C ₂₇ H ₃₀ O ₁₆	13.41	35.96 ± 9.94ab	29.52 ± 1.82bc	32.52 ± 2.60b	20.53 ± 0.18cd	44.10 ± 1.66a	15.55 ± 0.04d	30.81 ± 2.27bc	30.29 ± 1.80bc
Quercetin	C ₁₅ H ₁₀ O ₇	19.34	5.89 ± 1.33bc	2.31 ± 0.10e	3.11 ± 0.09de	4.36 ± 0.23cd	3.24 ± 0.12de	7.64 ± 0.09a	5.71 ± 0.19bc	6.34 ± 0.76ab
3-O-Methyl quercetin	C ₁₆ H ₁₂ O ₇	21.00	3.18 ± 0.70a	0.41 ± 0.09d	1.15 ± 0.47cd	1.76 ± 0.08bc	0.57 ± 0.12d	3.16 ± 0.10a	2.47 ± 0.41ab	1.11 ± 0.24d
Kaempferol	C ₁₅ H ₁₀ O ₆	22.02	6.87 ± 0.57b	3.97 ± 0.35cd	9.30 ± 0.66a	0.60 ± 0.09e	3.44 ± 0.28d	1.17 ± 0.15e	4.91 ± 0.56c	0.98 ± 0.05e
Phenolic acids										
Gallic acid	C ₇ H ₆ O ₅	0.63	114.64 ± 12.00c	46.35 ± 5.35d	287.03 ± 5.32a	128.92 ± 7.44c	194.88 ± 11.45b	107.21 ± 5.21c	194.17 ± 12.24b	197.49 ± 24.09b
trans-Cinnamic acid	C ₉ H ₈ O ₂	13.70	7.02 ± 1.30a	2.69 ± 0.08b	0.71 ± 0.02d	5.74 ± 0.23a	2.54 ± 0.51bc	1.06 ± 0.60cd	2.27 ± 0.07bcd	7.10 ± 0.53a
Caffeic acid	C ₉ H ₈ O ₄	4.17	12.04 ± 0.80ab	12.97 ± 0.89a	11.41 ± 1.06ab	13.12 ± 1.68a	11.36 ± 0.81ab	7.88 ± 0.81c	10.79 ± 0.59ab	9.54 ± 0.24bc
Chlorogenic acid	C ₁₆ H ₁₈ O ₉	4.93	77.75 ± 5.57cde	137.31 ± 10.00a	66.07 ± 2.35e	96.94 ± 2.84b	71.10 ± 2.36de	43.99 ± 0.33f	91.20 ± 2.58bc	84.21 ± 5.99bcd
p-Coumaric acid	C ₉ H ₈ O ₃	5.41	21.14 ± 1.56de	12.83 ± 3.36f	11.06 ± 1.60f	26.25 ± 0.54bc	25.25 ± 1.44cd	20.26 ± 0.74e	30.53 ± 1.63b	36.16 ± 0.38a
trans-Ferulic acid	C ₁₀ H ₁₀ O ₄	7.58	5.09 ± 0.18a	3.72 ± 0.03c	3.06 ± 0.01d	3.95 ± 0.012bc	3.12 ± 0.04d	4.08 ± 0.06b	3.92 ± 0.05bc	3.89 ± 0.07bc
Stilbene										
trans-Resveratrol	C ₁₄ H ₁₂ O ₃	24.89	0.05 ± 0.00b	0.05 ± 0.00b	0.05 ± 0.00b	0.05 ± 0.00b	0.05 ± 0.02b	0.05 ± 0.00b	0.05 ± 0.00b	0.06 ± 0.00a
Flavone										
Luteolin	C ₁₅ H ₁₀ O ₆	19.96	3.27 ± 0.62b	1.70 ± 0.11d	1.88 ± 0.22d	2.03 ± 0.31cd	1.32 ± 0.04d	3.00 ± 0.24bc	4.77 ± 0.24a	5.21 ± 0.55a
Flavan-3-ol										
Catechin	C ₁₅ H ₁₄ O ₆	4.16	135.63 ± 33.66cd	82.98 ± 10.06ef	179.59 ± 19.93abc	117.54 ± 6.80de	159.38 ± 10.24bcd	61.60 ± 2.28f	225.20 ± 20.18a	209.82 ± 21.06ab
Hydroxytyrosol	C ₈ H ₁₀ O ₃	1.86	5.49 ± 1.77cd	6.26 ± 0.92cd	17.79 ± 0.15a	4.69 ± 0.59d	8.23 ± 1.09bc	1.26 ± 0.30e	5.31 ± 0.86cd	10.67 ± 2.07b
Totals										
Anthocyanins			222.56 ± 33.48bc	48.55 ± 1.33f	100.17 ± 7.11e	208.51 ± 4.93cd	168.17 ± 8.34d	179.40 ± 1.01cd	418.88 ± 20.19a	272.72 ± 24.60b
Flavonols			51.90 ± 11.82a	36.20 ± 1.93bc	46.09 ± 3.75ab	27.26 ± 0.41c	51.34 ± 1.98a	27.52 ± 0.08c	43.90 ± 3.17ab	38.71 ± 2.64abc
Phenolic acids			237.68 ± 8.60de	215.87 ± 18.98ef	379.35 ± 8.38a	274.93 ± 9.72cd	308.25 ± 6.88bc	184.48 ± 5.28f	332.88 ± 13.40b	338.39 ± 30.72ab
Stilbenes			0.05 ± 0.00b	0.05 ± 0.00b	0.05 ± 0.00b	0.05 ± 0.00b	0.05 ± 0.02b	0.05 ± 0.00b	0.05 ± 0.00b	0.06 ± 0.00a

Table 1. Continued

Metabolite	Molecular formula	RT (min)	Bordo	Isabel Precoce	Concord Cl 30	BRS Rúbea	BRS Cora	BRS Carmen	BRS Violeta	BRS Magna
Flavones			3.27 ± 0.62b	1.70 ± 0.11d	1.88 ± 0.22d	2.03 ± 0.31cd	1.32 ± 0.04d	3.00 ± 0.24bc	4.77 ± 0.24a	5.21 ± 0.55a
Flavan-3-ol			135.63 ± 33.66cd	82.98 ± 10.06ef	179.59 ± 19.93abc	117.54 ± 6.80de	159.38 ± 10.24bcd	61.60 ± 2.28f	225.20 ± 20.18a	209.82 ± 21.06ab
Total			656.58 ± 78.52c	391.61 ± 12.13d	724.92 ± 16.04c	635.05 ± 17.19c	696.74 ± 11.48c	457.31 ± 7.77d	1030.99 ± 42.43a	875.58 ± 79.35b
Monomeric anthocyanins			251.32 ± 6.48c	76.04 ± 31.50e	53.21 ± 4.68e	219.73 ± 15.41c	269.69 ± 19.53c	165.18 ± 24.87d	551.34 ± 12.76a	441.41 ± 15.31b

Note: Distinct lettering corresponds to statistically significant differences in the rows, Tukey's HSD $P < 0.05$. Undetected metabolites are shown as a dash (—).

Phenolic compound analyses by ultra-high-performance liquid chromatography (UHPLC)

Phenolic compounds were identified and quantified by UHPLC, according to a modified protocol based on da Silva *et al.*,²² using an Ultimate 3000 BioRS Dionex (Thermo Fisher Scientific Inc., Waltham, MA, USA) system, equipped with Acclaim TM RSLC 120 C18 columns (2.2 μm , 2.1 mm \times 50 mm; Thermo Scientific), coupled with a diode array detector, operating at 280, 320, 360, and 520 nm.

Juice samples were membrane-filtered (polytetrafluoroethylene (PTFE) 0.45 μm ; Millipore, Burlington, MA, USA), and 20 μL was injected. The mobile phase consisted of ultrapure water with phosphoric acid 0.85% (A) and HPLC-grade acetonitrile (B). Metabolites were eluted by gradient, starting at 100% solvent A, decreasing from 96% A in 2.5 min, 92% A in 7.5 min, 88% A in 15 min, 85% A in 18 min, 80% A in 20 min, 35% A in 24 min, maintained up to 25 min, with a final increase to 100% A in 28 min, at a flow of 0.8 mL min^{-1} . The compounds were identified by comparison with commercial standards (gallic acid, catechin, *trans*-cinnamic acid, caffeic acid, chlorogenic acid, *p*-coumaric acid, *trans*-ferulic acid, *trans*-resveratrol, rutin, quercetin, luteolin, hydroxytyrosol, 3-*O*-methyl-quercetin, kaempferol, cyanidin-3,5-diglucoside, delphinidin-3-*O*-glucoside, cyanidin-3-*O*-glucoside, pelargonidin-3-*O*-glucoside, malvidin-3,5-diglucoside, peonidin-3-*O*-glucoside, and malvidin-3-*O*-glucoside), purchased from Sigma-Aldrich (St Louis, MO, USA). Standards were selected based on the compounds identified in previous studies with wines, from the cultivars.^{23–25} HPLC-grade acetonitrile was acquired from Tedia Laboratory Products (Rio de Janeiro, Brazil). Metabolite quantification was performed by the external standard method using calibration curves prepared with commercial standards.

Volatile compound extraction and identification by gas chromatography–mass spectrometry (GC-MS)

Volatile metabolites were captured by solid-phase microextraction (SPME) and analyzed using a QP-5000 gas chromatograph (Shimadzu Corporation, Kyoto, Japan) coupled with a mass spectrometer with electron impact ionization (70 eV). A total of 3 g NaCl was added to 10 mL juice sample in a 35 mL glass flask with screw cover and septum. The mixture was incubated under constant agitation at 30 °C for 30 min. Subsequently, the SPME fiber (CAR/DVB/PDMS, Supelco, Inc., Bellefonte, PA, USA) was exposed inside the vial (headspace) for 8 min. The fiber was retracted and exposed inside the chromatograph injector for desorption of the compounds. The temperature was set at 220 and 240 °C for the injector and detector, respectively. Helium was used as carrier gas, at 1 mL min^{-1} flow. Samples were injected in split 1/20 mode, and substances were separated on a DB-5 column (30 m \times 0.25 mm \times 0.25 μm), according to the following temperature program: from 35 to 240 °C, with 3 °C min^{-1} stepwise increases. Substance retention indices were determined by the injection of a homologous series of C8–C20 *n*-alkanes (Merck, St Louis, MO, USA), using the same chromatographic conditions as the samples, and calculated using the Van den Dool and Kratz equation.²⁶ Relative quantification was performed by the area normalization method. Each sample was analyzed in triplicate. Compound identification was performed by mass spectrometry and retention indices comparisons against the equipment library (Wiley 139, NIST 62) and literature data.²⁷

Juice analysis by UHPLC–MS

Juice samples were filtered through 0.45 μm PTFE membranes into MS-certified amber vials and an aliquot of 5 μL was injected.

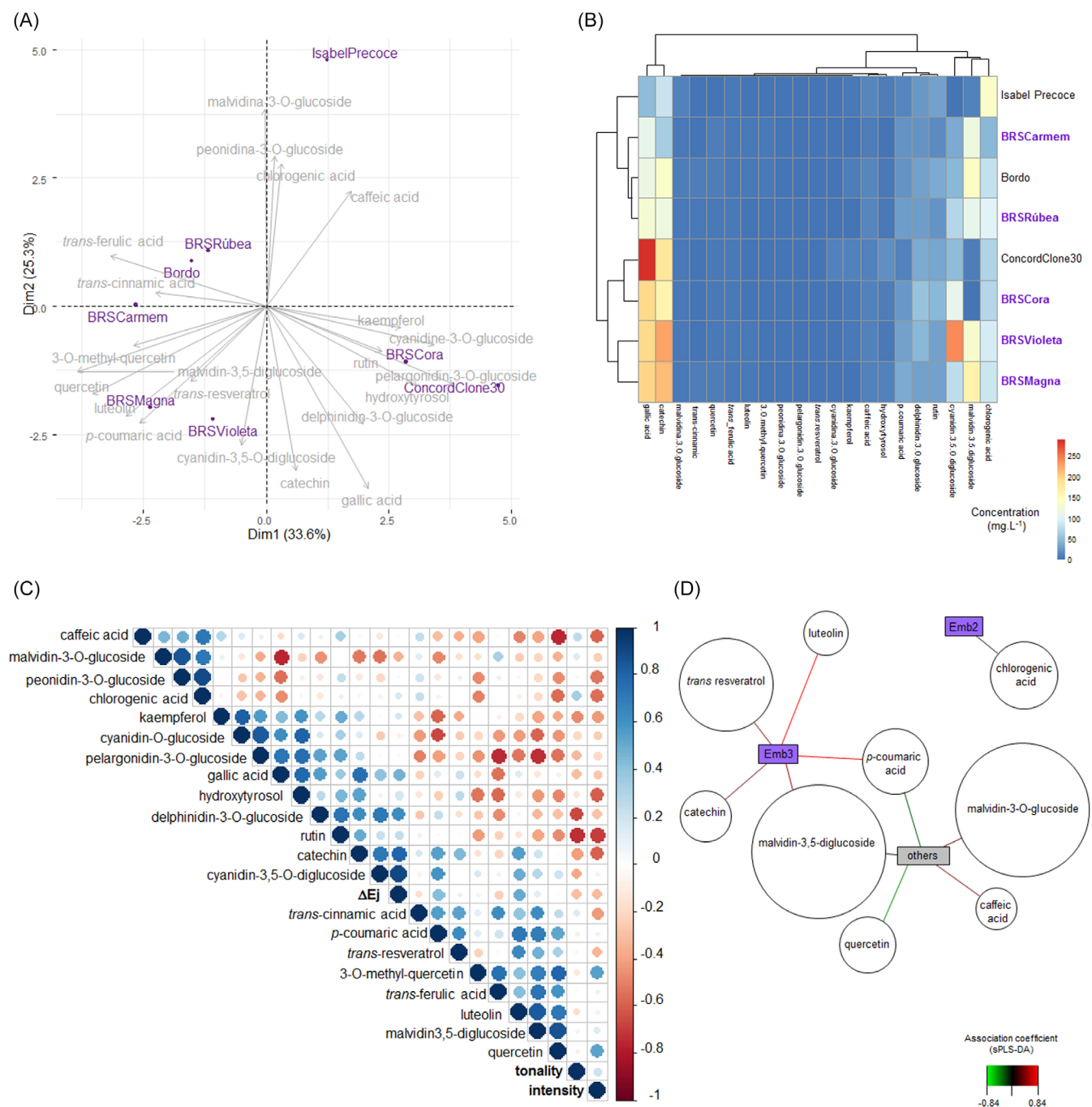


Figure 3. Profile of phenolic compounds in the juices. Principal component analysis (PCA) biplot (A) and hierarchical cluster analyses of metabolite levels (B). Correlation analyses between the contents of phenolic compounds and color parameters of the juices (C) and relevance network of phenolic compounds (cutoff = 0.75) (D).

The analytical method was performed using an ultra-high performance liquid chromatograph (Acquity, Waters Corporation, Milford, MA, USA) coupled with a triple quadrupole mass spectrometer (Acquity, Waters). Ionization was performed via electrospray in both negative and positive ion mode (ESI[±]) with capillary voltage ± 3.5 kV, cone ± 30 V, capillary temperature 150 °C and desolvation temperature 300 °C. The chromatographic conditions were a gradient elution using purified water with 0.1% formic acid as solvent A and acetonitrile (HPLC grade, Merck) as solvent B, with a C18 BEH Acquity column (1.7 μ m \times 2.1 mm \times 50 mm; Waters), flow 0.2 mL min⁻¹, and oven

temperature 40 °C. The gradient started with 5% B, ramped to 50% B in 8.00 min, and to 95% B in 9 min, held until 10.0 min, returned to the initial conditions at 10.1 min, and the column equilibrated until 12.0 min.

Statistical data analyses

One- and two-way analyses of variance (ANOVA) and multiple mean comparisons, using Tukey's *t*-test at *P* < 0.05, were carried out in R v. 4.2.0.¹⁷ Raw UHPLC-MS data from positive and negative modes were converted to mzXML using Proteowizard,²⁸ pre-processed, and further analyzed in R. Initially, the data were

Table 2. Profile of volatile metabolites from grape juices determined by GC-MS analyses. Relative contents are expressed as a percentage (%). Values represent means from three replicates per genotype \pm standard deviation ($n = 24$). Experimental linear-temperature-programmed retention indices (LTPRI) are shown

Metabolite	Molecular formula	LTPRI	Bordo	Isabel Precoce	Concord CI 30	BRS Rúbea	BRS Cora	BRS Carmen	BRS Violeta	BRS Magna
<i>Esters</i>										
Ethyl butanoate	C ₆ H ₁₀ O ₂	771	1.33 \pm 1.24 ^{a,b}	1.31 \pm 0.13 ^{a,b}	0.47 \pm 0.06 ^b	1.93 \pm 0.21 ^a	1.42 \pm 0.15 ^{a,b}	1.56 \pm 0.22 ^{a,b}	1.92 \pm 0.07 ^a	1.84 \pm 0.05 ^a
Ethyl methacrylate	C ₇ H ₁₂ O ₃	814	16.84 \pm 1.68 ^{e,f}	17.04 \pm 0.48 ^{d,e,f}	14.60 \pm 0.54 ^f	41.87 \pm 2.36 ^a	33.43 \pm 1.53 ^b	28.44 \pm 2.42 ^c	21.26 \pm 0.87 ^d	20.44 \pm 0.67 ^{d,e}
Ethyl isovalerate	C ₇ H ₁₄ O ₂	839	—	—	1.91 \pm 0.73 ^a	0.51 \pm 0.47 ^b	—	—	—	0.64 \pm 0.39 ^b
Isopentyl acetate	C ₇ H ₁₄ O ₂	861	—	—	0.82 \pm 0.17 ^a	0.85 \pm 0.36 ^a	—	—	—	0.51 \pm 0.02 ^a
Ethyl tiglate	C ₇ H ₁₂ O ₂	924	—	—	—	—	—	—	0.26 \pm 0.03 ^b	0.31 \pm 0.02 ^a
Ethyl hexanoate	C ₈ H ₁₆ O ₂	942	—	—	0.94 \pm 0.23 ^b	—	2.62 \pm 0.17 ^a	0.46 \pm 0.06 ^c	0.31 \pm 0.06 ^{c,d}	1.25 \pm 0.22 ^b
Hexyl acetate	C ₈ H ₁₆ O ₂	1014	—	—	5.32 \pm 0.29 ^a	—	—	0.48 \pm 0.05 ^b	—	0.37 \pm 0.01 ^b
Ethyl octanoate	C ₁₀ H ₂₀ O ₂	1192	—	—	—	—	—	—	—	0.59 \pm 0.12 ^a
Phenylethyl acetate	C ₁₄ H ₂₀ O ₂	1233	—	2.40 \pm 0.31 ^a	1.63 \pm 0.00 ^c	—	—	—	—	0.54 \pm 0.02 ^b
<i>Aldehydes</i>										
Furfural	C ₅ H ₄ O ₂	970	0.78 \pm 0.22 ^{b,c}	0.73 \pm 0.07 ^{b,c}	2.52 \pm 0.66 ^a	0.82 \pm 0.97 ^{b,c}	0.52 \pm 0.15 ^{b,c}	1.23 \pm 0.10 ^{b,c}	0.24 \pm 0.05 ^c	1.52 \pm 0.05 ^{a,b}
<i>n</i> -Decanal	C ₁₀ H ₂₀ O	1189	—	0.36 \pm 0.06 ^a	—	—	—	0.29 \pm 0.05 ^a	—	0.28 \pm 0.09 ^a
<i>Alcohols</i>										
3- <i>E</i> -Hexanol	C ₆ H ₁₄ O	776	—	0.65 \pm 0.11 ^c	0.99 \pm 0.16 ^c	1.60 \pm 0.02 ^{a,b}	9.65 \pm 0.01 ^{a,b}	10.94 \pm 0.91 ^a	3.56 \pm 0.37 ^{a,b}	4.06 \pm 0.10 ^{a,b}
2- <i>E</i> -Hexanol	C ₆ H ₁₄ O	784	8.38 \pm 0.88 ^{c,d}	19.05 \pm 0.31 ^a	12.02 \pm 0.33 ^{b,c}	3.87 \pm 3.75 ^e	13.20 \pm 1.43 ^b	4.92 \pm 0.51 ^{d,e}	14.14 \pm 0.72 ^b	13.20 \pm 0.31 ^b
<i>n</i> -Hexanol	C ₆ H ₁₄ O	803	19.35 \pm 2.04 ^c	30.31 \pm 0.58 ^b	34.66 \pm 1.35 ^b	10.84 \pm 0.20 ^d	21.86 \pm 0.83 ^c	37.85 \pm 3.21 ^{a,b}	42.33 \pm 0.75 ^a	42.31 \pm 0.88 ^a
2-Heptanol	C ₇ H ₁₆ O	1009	—	—	0.50 \pm 0.06 ^{a,b}	0.52 \pm 0.05 ^a	—	0.40 \pm 0.05 ^{b,c}	0.33 \pm 0.07 ^c	0.40 \pm 0.04 ^{b,c}
3- <i>Z</i> -Heptanol	C ₇ H ₁₆ O	1019	—	—	—	—	—	—	—	0.28 \pm 0.07 ^a
1-Octen-3-ol	C ₈ H ₁₆ O	972	0.59 \pm 0.07 ^b	0.32 \pm 0.03 ^c	0.92 \pm 0.04 ^a	0.36 \pm 0.13 ^c	0.32 \pm 0.06 ^c	—	0.62 \pm 0.06 ^b	0.47 \pm 0.04 ^{b,c}
2-Ethyl hexanol	C ₈ H ₁₈ O	1048	5.39 \pm 0.79 ^a	1.24 \pm 0.05 ^{b,c}	0.62 \pm 0.10 ^{c,d}	1.83 \pm 0.62 ^b	—	0.78 \pm 0.10 ^{c,d}	—	0.97 \pm 0.10 ^{b,c,d}
1-Octanol	C ₈ H ₁₈ O	1057	2.03 \pm 0.17 ^a	0.56 \pm 0.02 ^b	1.81 \pm 0.20 ^a	0.91 \pm 0.47 ^b	0.65 \pm 0.37 ^b	0.27 \pm 0.04 ^b	0.58 \pm 0.17 ^b	0.35 \pm 0.02 ^b
2-Phenyl ethanol	C ₈ H ₁₀ O	1086	3.58 \pm 0.91 ^a	2.75 \pm 0.92 ^a	0.69 \pm 0.10 ^b	1.85 \pm 1.33 ^{a,b}	—	0.34 \pm 0.07 ^b	—	0.38 \pm 0.15 ^b
1-Nonanol	C ₉ H ₂₀ O	1149	0.64 \pm 0.39 ^a	—	—	—	—	—	—	0.27 \pm 0.09 ^{a,b}
<i>Ketones</i>										
2-Heptanone	C ₇ H ₁₄ O	871	7.21 \pm 1.17 ^a	0.90 \pm 0.04 ^{b,c}	2.17 \pm 0.05 ^{b,c}	3.91 \pm 3.06 ^b	9.27 \pm 0.29 ^a	0.24 \pm 0.02 ^c	3.69 \pm 0.31 ^b	0.25 \pm 0.01 ^c
1-Octen-3-one	C ₈ H ₁₄ O	956	5.78 \pm 1.81 ^a	1.39 \pm 0.21 ^{b,c}	4.12 \pm 0.10 ^{a,b,c}	4.32 \pm 2.67 ^{a,b}	1.09 \pm 0.15 ^{b,c}	0.80 \pm 0.07 ^c	1.11 \pm 0.81 ^{b,c}	1.37 \pm 0.08 ^{b,c}
2-Octanone	C ₈ H ₁₆ O	964	1.03 \pm 0.24 ^a	0.39 \pm 0.03 ^{b,c}	0.60 \pm 0.08 ^b	0.44 \pm 0.17 ^{b,c}	0.44 \pm 0.05 ^{b,c}	—	0.26 \pm 0.09 ^{c,d}	—
Damascenone	C ₁₃ H ₁₈ O	1361	—	—	—	—	—	—	—	0.27 \pm 0.04 ^a
<i>Alkenes</i>										
1-Decene	C ₁₀ H ₂₀	987	—	0.49 \pm 0.06 ^b	0.73 \pm 0.13 ^a	—	—	0.21 \pm 0.05 ^c	0.20 \pm 0.06 ^c	0.50 \pm 0.03 ^b
<i>cis</i> -Ether-decadiene	C ₁₀ H ₁₈	1117	—	—	—	—	—	—	—	0.23 \pm 0.01 ^a
<i>Acids</i>										
2-Hexanoic acid	C ₁₄ H ₁₅ NO ₄	1053	1.25 \pm 0.29 ^{b,c}	2.70 \pm 0.17 ^a	1.46 \pm 0.12 ^{b,c}	1.89 \pm 0.72 ^{a,b}	1.16 \pm 0.17 ^{b,c}	0.79 \pm 0.14 ^c	1.33 \pm 0.04 ^{b,c}	1.44 \pm 0.04 ^{b,c}
<i>Monoterpenes</i>										
α -Terpineol	C ₁₀ H ₁₈ O	1209	6.19 \pm 1.26 ^{a,b}	10.65 \pm 0.90 ^a	4.63 \pm 0.51 ^{b,c}	7.00 \pm 4.91 ^{a,b}	—	0.81 \pm 0.08 ^c	0.87 \pm 0.13 ^c	0.73 \pm 0.12 ^c

Table 2. Continued

Metabolite	Molecular formula	LTPRI	Bordo	Isabel Precoce	Concord Cl 30	BRS Rúbea	BRS Cora	BRS Carmen	BRS Violeta	BRS Magna
<i>neo</i> -iso-3-Thujyl acetate	C ₁₂ H ₂₀ O ₂	1251	2.03 ± 0.60a	1.40 ± 0.25a ^{bc}	—	1.61 ± 0.39a ^b	1.65 ± 0.40a ^b	0.84 ± 0.13b ^{cd}	0.57 ± 0.06c ^d	0.60 ± 0.05c ^d
Totals										
Esters			18.17 ± 2.74f	20.75 ± 0.88e ^f	24.06 ± 0.65d ^e	45.16 ± 2.80a	37.47 ± 1.31b	30.94 ± 2.69c	25.26 ± 0.50d ^e	26.48 ± 0.47c ^d
Aldehydes			0.78 ± 0.22b ^{cd}	1.09 ± 0.13b ^{cd}	2.52 ± 0.66a	0.82 ± 0.97b ^{cd}	0.52 ± 0.15c ^d	1.52 ± 0.13a ^{bc}	0.24 ± 0.05d	1.80 ± 0.04a ^b
Alcohols			39.95 ± 3.14a	54.89 ± 0.19a	52.20 ± 1.46a	21.78 ± 0.53a	45.68 ± 1.77a	55.49 ± 4.67a	61.55 ± 0.40a	62.67 ± 1.01a
Ketones			14.02 ± 3.19a	2.67 ± 0.24c ^d	6.89 ± 0.19b ^{cd}	8.66 ± 5.89a ^{bc}	10.80 ± 0.37a ^b	1.04 ± 0.09d	5.06 ± 0.45b ^{cd}	1.89 ± 0.10c ^d
Alkenes			—	0.49 ± 0.06b	0.73 ± 0.13a	—	—	0.21 ± 0.05c	0.20 ± 0.06c	0.73 ± 0.03a
Acids			1.25 ± 0.29b ^c	2.70 ± 0.17a	1.46 ± 0.12b ^c	1.89 ± 0.72a ^b	1.16 ± 0.17b ^c	0.79 ± 0.14c	1.33 ± 0.04b ^c	1.44 ± 0.04b ^c
Monoterpenes			8.66 ± 0.79a ^b	13.06 ± 0.96a	5.22 ± 0.52b ^c	10.00 ± 5.77a ^b	1.65 ± 0.40c	2.18 ± 0.19c	2.27 ± 0.11c	2.19 ± 0.19c

Note: Distinct lettering corresponds to statistically significant differences in the rows, Tukey's HSD $P < 0.05$. Undetected metabolites are shown as a dash (—).

optimized using the package IPO,²⁸ pre-processed with XCMS^{28,29} into one table for each ionization mode (ES+ and ES–), resulting in 34 and 169 mass features for the positive and negative modes, respectively. The mass features were analyzed using the web-based MetaboAnalyst software.³⁰ Correlation analyses and plots were performed with normalized color and UHPLC data, using the packages Hmisc³¹ and corplot.³² Scaled and centered UHPLC, GC-MS and UHPLC–MS data were used in multivariate analyses using the packages FactoMineR,³³ factoextra³⁴ and mixOmics.³⁵ Sparse partial least square (sPLS) analyses were carried out using pedigree information as discriminant (DA), considering three levels of Embrapa genotypes and cultivars from other sources. Relevance association networks were calculated from a similarity matrix obtained from the sum of the correlations between the original variables and each of the latent components of the sPLS model. The cut-off values correspond to the tuning threshold for the relevant associations network. Agglomerative hierarchical clustering was carried out by maximum likelihood estimation and Bayesian modeling using the package mclust.³⁶ Optimal models were determined according to BIC (Bayesian information criterion) and EM (expectation–maximization) criteria, as parameters in the Gaussian mixture model. Genetic distance and chemical profile matrices were compared using canonical co-inertia analysis, using the package ade4.³⁷

RESULTS

The metabolic and genetic profiles were determined for grape juices obtained from the traditional cultivar 'Bordo/lves', mutation clones from 'Concord' and 'Isabella', 'Concord Clone 30' and 'Isabel Precoce', selected based on precocious berry ripening and phenological cycle, respectively, and five cultivars developed by controlled crosses. Typical clusters of 'BRS Rúbea', 'BRS Cora', 'BRS Carmem', 'BRS Violeta', and 'BRS Magna' are shown in Fig. 1(A–E). Genotypic characterization of the cultivars using a 14-SSR marker set confirmed the mutation status of 'Isabel Precoce' and 'Concord Clone 30' (Fig. 1(F–G)). The genetic distance between the investigated cultivars ranged from 0.13 ('Bordo' to 'BRS Rúbea') to 0.45 ('Isabel Precoce' to 'BRS Magna') (Fig. 1(G)). The high genetic similarity among the grapevine juice genotypes reflects the shared parentage among them (Fig. 1(G); Supporting Information, Figs S1 and S2). The number of alleles per marker ranged from 3 (VVM25) to 9 (ssrVrZAG112), the expected and observed heterozygosity from 0.44 (VVM25) to 0.87 (VVM36), and 0.55 (ssrVrZAG83, VVM27, VVM25, SSR112) to 1 (VVM36), respectively (Fig. S2). The set of markers produced an average PIC of 0.48 and an accumulated probability of identity of 6.35×10^{-8} .

Physicochemical and color properties

The contents of soluble solids, total phenolic compounds, and anthocyanins were generally higher in juices from the newly developed cultivars, particularly in the most recent group ('BRS Violeta' and 'BRS Magna') (Fig. 2(A–D)). Principal component analysis (PCA) demonstrated that a large part of the overall variation (99.7%) in the physicochemical properties of the juices, including the ratio between the contents of soluble solids and titratable acidity, was explained by differences among the genotypes (Supporting Information, Fig. S3A), although a significant effect of the environment (vintage) is observed for SSC, TPI and total anthocyanins (ANT) (Supporting Information, Table S2).

The SSC in the juices ranged from 15.2 to 18.4 °Brix in ‘Concord Clone 30’ and ‘BRS Rúbea’ and ‘Isabel Precoce’, respectively (Fig. 2 (A)). The juices with higher titratable acid levels were from ‘Bordo’ and ‘Concord Clone 30’, whereas ‘BRS Magna’ was the least acidic (Fig. 2(B)). ‘BRS Violeta’, and to a lesser extent ‘BRS Magna’, exhibited higher contents of total phenolics and anthocyanins (Fig. 2(C, D)). In contrast, juices from ‘Isabel Precoce’ had low levels of total phenolics despite the relatively high ANT content (Fig. 2(C,D)).

The color of the juices from the investigated cultivars was different from the ‘Bordo/Ives’ standard, with ‘Concord Clone 30’ and ‘BRS Violeta’ exhibiting the greatest overall difference (Supporting Information, Fig. S3B). Color intensity and tonality contributed most to the observed differences, with ‘BRS Violeta’ displaying the most intense color and ‘BRS Magna’ the higher ratio between violet and green (Fig. S3B). The saturation of color, determined as CIELAB chroma, was not significantly different among the samples.

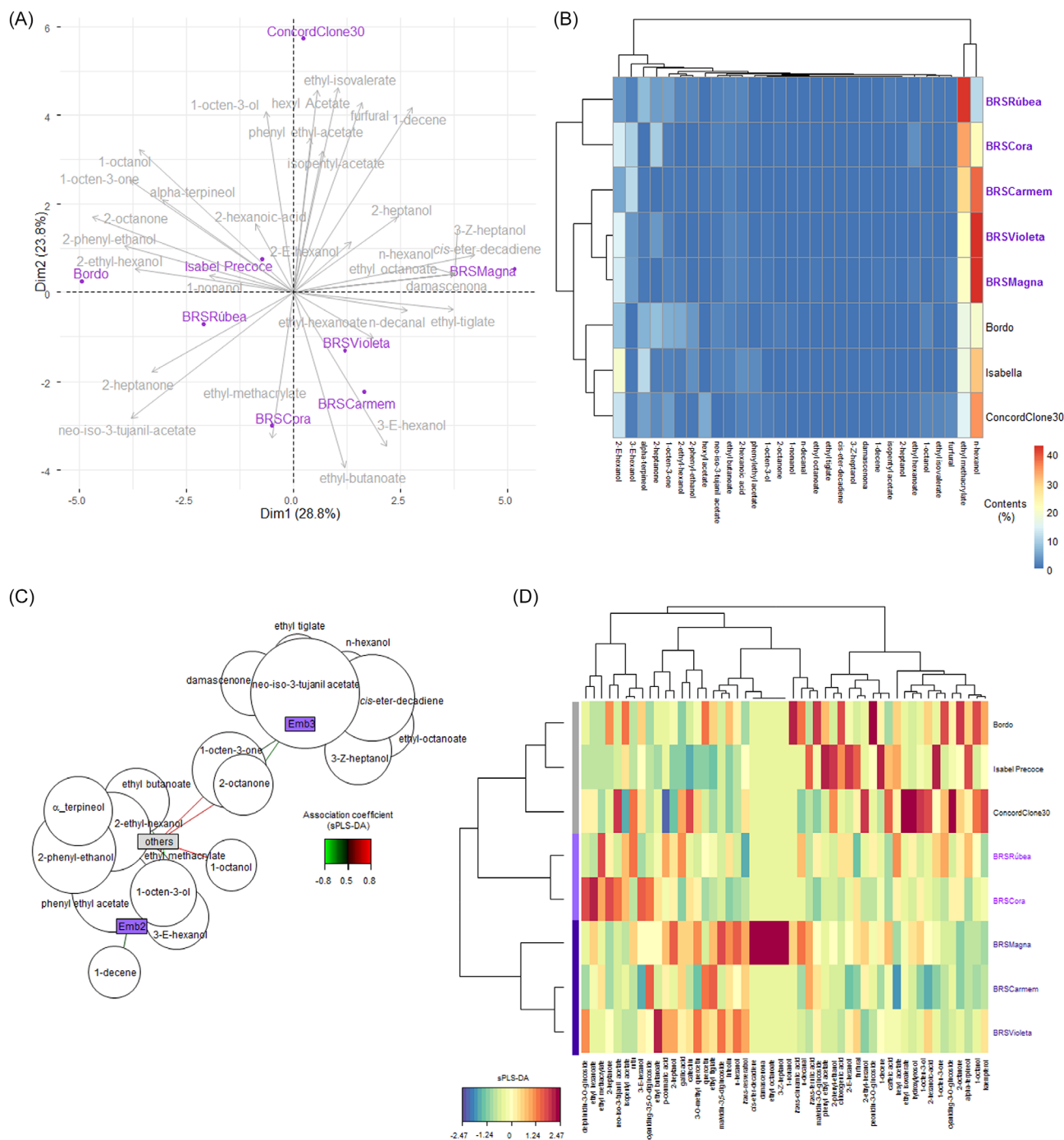


Figure 4. Profile of volatile metabolites in the juices. Principal component analysis (PCA) biplot (A) and hierarchical cluster analyses of the metabolite levels (B). Relevance network of volatile compounds (cutoff = 0.55) (C) and clustered image map (CIM) of the sparse partial least squares discriminant analyses (sPLS-DA) model of the profiles of volatiles in the juices (D).

Phenolic compound profile

A total of 21 distinct phenolic metabolites from six chemical classes – anthocyanins, flavonols, phenolic acids, stilbene, flavone, and flavan-3-ols – were identified in the juices from the eight cultivars (Table 1). Anthocyanin contents were significantly higher in juices from 'BRS Violeta', whereas levels of *trans*-resveratrol were similar in all juices, with slightly higher content in 'BRS Magna' (Table 1, Fig. 3). Multivariate PC analyses evidenced a variation higher than 58% in the phenolics composition of the juices, with greater contributions from 'BRS Violeta', 'BRS Magna', and 'BRS Cora', and lower from 'Isabel Precoce' (Fig. 3(A)). Among the phenolic metabolites, flavan-3-ols, anthocyanins, and phenolic acids contributed most to the overall variation among the juices (Supporting Information Fig. S3B). Hierarchical clustering revealed two groups of juices: one consisting of 'Isabel Precoce', 'BRS Carmem', and 'Bordo', and the other characterized by higher contents of catechin and gallic acid, consisting of 'Concord Clone 30', 'BRS Cora', 'BRS Violeta', and 'BRS Magna' (Fig. 3(B)). Juices from 'BRS Violeta' and 'BRS Magna' were also characterized by high contents of diglycosidic anthocyanins and chlorogenic acid (Fig. 3(B)).

The contents of catechin and cyanidin-3,5-*O*-diglucoside were positively correlated with the total difference in color among the juices, whereas levels of rutin were negatively correlated with tonality and color intensity (Fig. 3(C); Supporting Information, Table S3). Overall differences in color were also positively correlated with the levels of delphinidin-3-*O*-glucoside and gallic acid, although at lower significance levels (Fig. 3(c); Table S3). The network of relevant associations obtained from the canonical correlation analysis and sparse PLS regression between the groups of genotypes and the contents of phenolic metabolites demonstrated a positive association of luteolin, catechin, and *trans*-

resveratrol to the most recent group of genotypes, 'BRS Violeta' and 'BRS Magna' (Fig. 3(D)). The group also exhibited a positive significant association with the contents of malvidin-3,5-diglucoside and *p*-coumaric acid, whereas these associations are negative for the group consisting of the genotypes 'Bordo', 'Isabel Precoce', and 'Concord Clone 30' (Fig. 3(D)). Caffeic acid levels are positively associated with the most recent cultivars.

Volatile compound profile

The volatile profile of the investigated juices comprised 30 metabolites from five chemical classes, including esters, aldehydes, alcohols, ketones, alkenes, acids, and monoterpenes (Table 2). The most complex mixture of volatiles was identified in juices from 'BRS Magna', with 29 metabolites, whereas the simplest was found in 'BRS Cora' with 14 compounds and 'Bordo', with 16 (Table 2). The esters and alcohols were the classes contributing most to the diversity of volatiles in 'BRS Magna' (Table 2; Fig. 4(A)). The total variation in the volatiles profile among the juices was 52.6%, with the principal component contributing 28.8% (Fig. 4(A)). The second principal component contributed most to the qualitative variation of the profiles of volatile metabolites.

Hierarchical clustering further separated the juices fingerprints of volatiles in three groups, consisting of two clusters of Embrapa genotypes – one with 'BRS Rúbea' and 'BRS Cora', and the other with 'BRS Carmem', 'BRS Violeta', and 'BRS Magna' – and one with the cultivars from other origins (Fig. 4(B)). Juices in the latter two groups were characterized by higher contents of hexanol-derived metabolites, synthesized from the lipoxygenase pathway (Fig. 4(B)). The relevance network for the volatile metabolites in the juices also revealed a more diverse chemical signature for the most recent group of cultivars ('BRS Violeta' and 'BRS Magna'), whereas the intermediate group ('BRS Cora' and 'BRS Carmem')

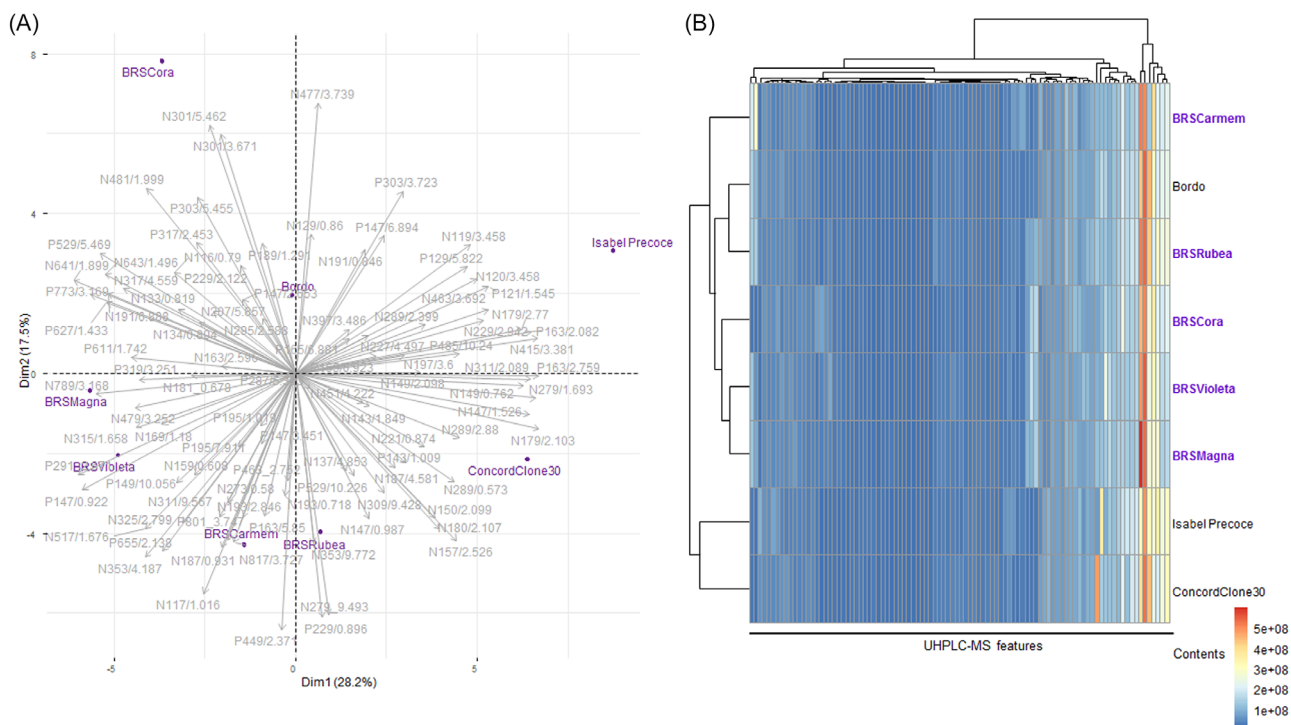


Figure 5. Untargeted metabolome profile of the juices. Principal component analysis (PCA) biplot (A) and hierarchical cluster analyses of the features levels (B).

exhibited a closer association with the profile of the cultivars from other origins (Fig. 4(C)). The eight carbon ketones were significantly associated with the 'Violeta/Magna' and 'other origin' groups of genotypes, although negatively with the first and

positively with the later. The intermediate group of Embrapa genotypes and those from other origins exhibited a similar network of relevant volatiles, except for 1-decene that was negatively associated with the 'Cora/Carmem' group (Fig. 4(C)).

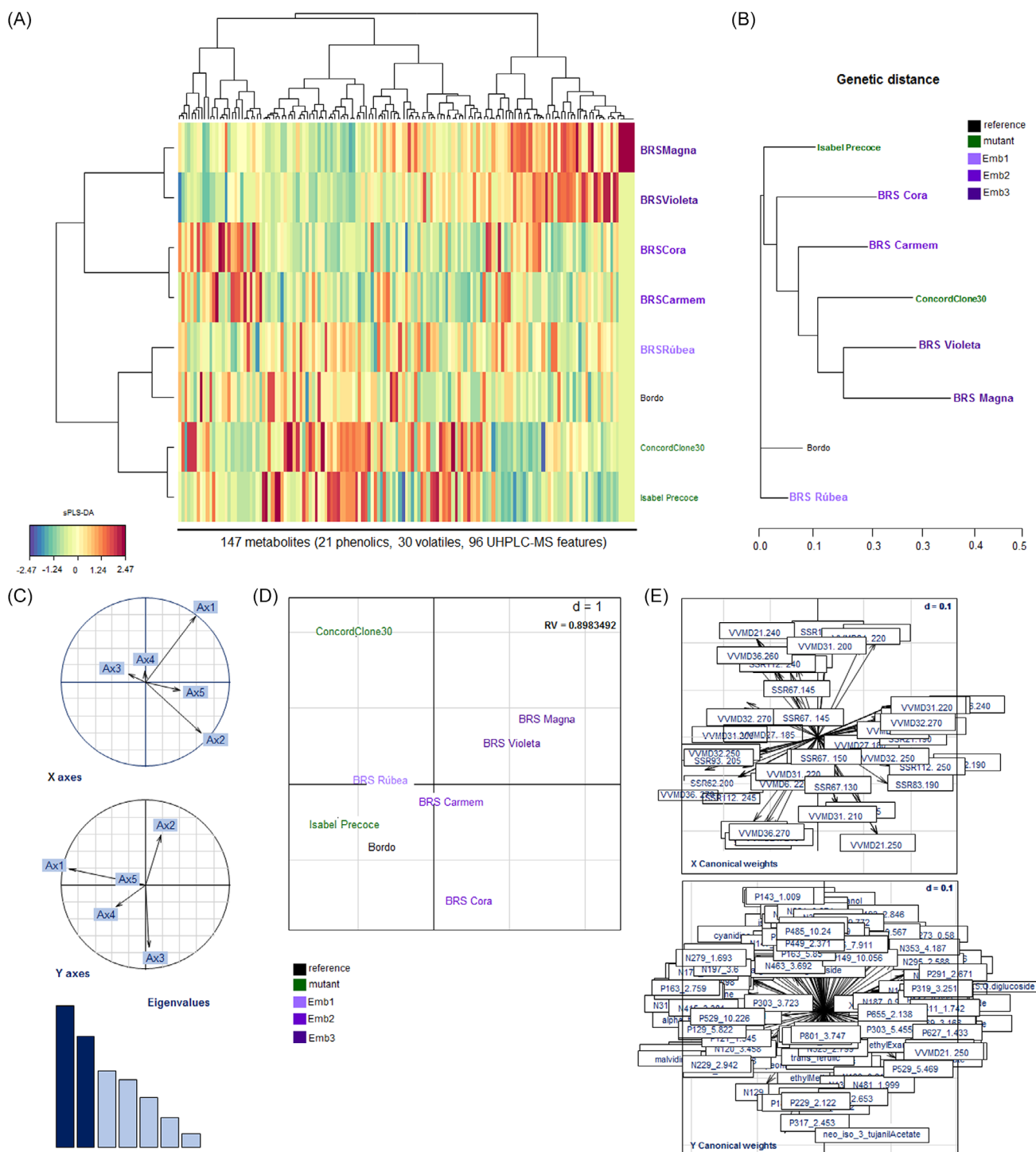


Figure 6. Comparison between juices' chemical signatures and grapevine cultivars' genetic distances. Clustered image map (CIM) of the sparse partial least squares discriminant analyses (sPLS-DA) model of the juices' metabolic profiles (A) and dendrogram representation of the genetic distance (B). Canonical co-inertia analyses of the juice chemical profile and genetic distance between the grapevine cultivars. Cumulative projected inertia (%) for x- and y-axis and eigenvalues decomposition (C). Projected co-inertia between the chemical profile of the juices and genetic distance between the cultivars (D). Canonical weights of the genetic (x) and chemical (y) variables (E). RV coefficient is based on 999 replicates (simulated P -value 0.092).

The phenolic and volatile profiles of the juices were integrated and analyzed using a sparse version of the multivariate partial least square analyses, using the genotype origins as discriminant (sPLS-DA). The analysis makes a sparsity assumption, which means that it considers that only a small number of features are responsible for driving a biological event or effect. Therefore, the methodology is effective for the analyses of highly dimensional data, where the number of features is much higher than the number of samples, as occurs often in metabolomics investigations. The integrated profile revealed three distinct clusters of chemical signatures for phenolic and volatile metabolites: one consisting of juices from other origins and one from the later genotypes developed at Embrapa, namely 'BRS Magna', 'BRS Violeta' and 'BRS Carmem'. Juices from 'BRS Rúbea' and 'BRS Cora' clustered together, with closer similarity to those from 'Bordo', 'Concord Clone 30', and 'Isabel Precoce' (Fig. 4(D)). Sample clustering using data from the integrated chemical profile gives rise to distinct associations in comparison to those obtained using the isolated phenolic or volatile compounds profile.

UHPLC-MS metabolomics profile and integrative analyses

UHPLC-MS profiling of the juices from the eight cultivars investigated in the current study led to the extraction of 96 features – 34 and 62 from the ESI positive and negative ion modes, respectively – from the UHPLC-MS chromatograms. Approximately 45% of the variation in the UHPLC-MS chemical profile of the juices was explained by the first (28.2%) and second (17.5%) PCs (Fig. 5(A)). Model-based clustering of the chemical profiles revealed the more divergent chemical profile of 'Concord Clone 30' and 'Isabel Precoce', in comparison to the other juice samples (Fig. 5(B)). The juices from the more recent group of cultivars ('Violeta'/'Magna') had a UHPLC-MS profile closer to that from 'BRS Cora', whereas the composition of juices from 'BRS Rúbea' was more similar to 'Bordo', with 'BRS Carmem' being the most divergent in the cluster (Fig. 5(B)). The contribution of the critical UHPLC-MS features to the first and second dimension for each group of cultivars in sPLS-DA is shown in Supporting Information, Fig. S4A. The most significant (cutoff = 0.75) associations between the metabolic features and the groups of cultivars is shown as relevance networks, displaying the negative association of the juices from the second and third group of genotypes to the features N309/9.428, N191/0.846, and P129/5.822, and positive to N134/0.804, P317/2.453, and P291/2.671 (Supporting Information, Fig. S3B). The contents of the UHPLC-MS features N149/0.762, N179/2.77, N179/2.103, N311/2.089, N415/3.381, N279/1.693, P163/2.759, and P163/2.082 were positively associated with the juices from the cultivars of other origins (Fig. S4B).

The UHPLC-MS data were integrated with the profiles of phenolic and volatile compounds of the juices from the eight cultivars and analyzed by sPLS-DA, using the genetic origin as discriminant. The metabolite profile of juices from 'BRS Rúbea' was closer to that from 'Bordo', whereas the samples from 'Concord Clone 30' and 'Isabel Precoce' were more divergent (Fig. 6(A); Supporting Information, Fig. S5A). The overall chemical profile of the juices from the second and third group of cultivars developed at Embrapa is significantly distinct than that from the initial parent line 'BRS Rúbea' and cultivars from clonal selection and other genetic origins (Fig. 6(A,B); Fig. S5A). The relevance network exhibiting the association between the classes of metabolites and groups of cultivars is shown in Supporting Information, Fig. S5B.

The genetic and chemical data were compared using canonical co-inertia analyses, which create a common ordination based on

the covariances of the compared data, to plot the variables in the same space, thus, revealing trends between the distinct datasets. The co-inertia analysis, carried out with 999 permutations, demonstrated that the overall juice chemical profile is related to the genetic distance between the cultivars, with an RV coefficient higher than 0.89 (Fig. 5(C–E)). The genetic association between the cultivars and the overall similarity in the chemical composition of the juices are retained in the common multivariate ordination generated by co-inertia (Fig. 5(D)).

DISCUSSION

The study investigated the effect of the genetic distance on the physicochemical properties and metabolic profile of juices from two phenological mutants of traditional cultivars and five novel varieties, generated by controlled crosses from three generations of a breeding program, during five successive vintages. Vintage significantly affects the physicochemical properties of the juices, especially the contents of sugar, phenolic compounds, and total anthocyanin. Previous comprehensive works also have demonstrated the effect of the environment on the sensory properties of grape and its derived products.^{38–42} A significant improvement of the juice contents in soluble solids, total phenolics, and total anthocyanins was detected in the new cultivars, regardless of the environmental effect. The increase in these compounds is a consequence of selection for the traits, as shown by the higher levels of sugars (~20%) and color-related metabolites (~67% and 35%, for phenolics and anthocyanins, respectively) in the most recent cultivars in comparison with the initial one. In grapes, phenolic compounds concentrated in the skin and seeds are critical constituents of the juice, due to their flavor and health-related properties.^{43–45} As shown in previous studies, the main phenolic metabolites in the juices were flavonoids (anthocyanins, flavanols, flavone, flavonols, and flavan-3-ols), and non-flavonoid (phenolic acids and stilbene) metabolites.^{23,43} The phenolic signature of the juices changed with the development of novel cultivars, as the parental 'BRS Rúbea' exhibited a profile similar to 'Bordo', and 'BRS Violeta' and 'BRS Magna' had higher contents of quercetin, 3-O-methyl-quercetin, luteolin, *p*-coumaric acid, of the anthocyanins cyanidin- and malvidin-3,5-O-diglucoside, and the stilbene *trans*-resveratrol. Correlation analyses highlighted the negative effect of the contents of phenolic acids, rutin, and catechin on the juice color intensity and tonality, as observed in juices from the Turkish variety 'Kalecik karasi'.⁴³ Catechin and gallic acid were also positively correlated with the total difference in juice colors, along with the contents of the anthocyanins cyanidin-3,5-O-diglucoside and delphinidin-3-O-glucoside. Relevance network analyses demonstrated the positive association of malvidin-3-O-glucoside and gallic acid with the juices from 'Bordo', 'Concord Clone30', and 'Isabel Precoce', whereas the most recent Embrapa cultivars were positively associated with metabolites luteolin, *trans*-resveratrol, and *p*-coumaric acid, demonstrated to have positive effects on health aspects.^{44–46} In agreement with our results, wines from five selections of two segregating populations, obtained from crosses between 'Monastrell' and 'Cabernet Sauvignon' or 'Syrah', also exhibited higher contents of catechin polymers.¹² The authors highlight the potential of breeding to improve wine sensory properties, namely, softness, by elevating the content of epigallocatechin.¹²

The profile of juice volatiles was also divergent between the traditional and the novel grape cultivars, although juices from 'Concord Clone 30' also displayed a distant volatile signature from

'Bordo' and 'Isabel Precoce'. The contents of esters were higher in the juices from Embrapa cultivars, whereas the contents of aldehydes and ketones were similar in all samples. Juices from 'BRS Magna', 'BRS Rúbea', and 'Concord Clone 30' exhibited the most complex blends of volatiles. Relevance network analyses demonstrate the most divergent profile of volatiles in the most recent cultivars, due to their differential association with metabolites derived from the lipoxygenase (LOX) pathway, negative for octanone and octen-3-one. The abundance of these metabolites, derived from the enzymatic breakdown of unsaturated fatty acids, contributed negatively to the sensory classification of berries from *vinifera* genotypes of table grapes.⁴⁷ Higher contents of terpenoids, in a muscat genotype, favored its acceptance and induced higher aroma ratings.⁴⁷ In our study, juices from 'Isabel Precoce', which has a larger contribution of *V. vinifera* in its pedigree, exhibited higher contents of terpenoids. Interestingly, juices from 'BRS Rúbea', with a predominant *V. labrusca* genomic context, had the second highest content of monoterpenes. Berries from a morphological mutant genotype of 'Glera', a traditional prosecco wine cultivar, also displayed a distinct profile of monoterpenes, due to higher levels of glycosidic linalool and nerol.¹³ Interestingly, selected clones of the cultivar did not exhibit significant chemical variation in volatiles and polyphenols.¹³

In a study comparing the volatiles from a *V. labrusca* × *V. vinifera* hybrid and a pure *V. vinifera* cultivar, esters were only detected in the volatiles of the hybrid cultivar.⁴⁸ The study also demonstrated a limited amount and diversity of terpenes in berries from the hybrid cultivar, which was associated with lower levels of expression of the genes encoding enzymes in the methylerythritol 4-phosphate pathway.⁴⁸ The profile of volatiles from berries of 'Hutai-8', a Chinese hybrid *Vitis vinifera* × *V. labrusca* cultivar, also had significant contributions of β -damascenone, hexanal, (*E*)-2-hexenal, (*E,Z*)-2,6-nonadienal, (*E*)-2-nonenal, and ethyl octanoate.⁴⁹ In *V. vinifera* cv. 'Marselan', the contents of LOX-derived volatiles 2-heptanol, *cis*-7-decenal, and *trans*-2-hexenal were not significantly influenced by shading, although the expression levels of genes encoding LOX oxidases, fatty acid hydroperoxide lyases, and alcohol dehydrogenases were shown to be highly correlated with volatile contents.⁵⁰ In contrast, leaf removal during fruit set increased the contents of monoterpenes and C₁₃-norisoprenoids in 'Xynisteri' grapes, a traditional *vinifera* cultivar from Cyprus.⁵¹

Recently, plant phenotyping has incorporated high-throughput metabolomics to genetic and system biology studies to bridge the gap between the genome and the phenotype.⁵² UHPLC-MS is considered a powerful tool and a comprehensive analytical approach in plant metabolomics due to its ability to separate metabolites in the liquid phase without pre-treatment.⁵³ However, metabolite annotation remains challenging due to the lack of standard tandem mass spectra for most plant metabolites.⁵² In our study, clustering analyses of UHPLC-MS features found in the investigated grape juices demonstrated the most divergent profile of 'Concord Clone 30' and 'Isabel Precoce'. The metabolome obtained by UHPLC-MS reflected the 'Bordo' parentage of 'BRS Rúbea' and the sibling relationship between 'BRS Violeta' and 'BRS Magna'. In contrast, the other group of sibling cultivars – 'BRS Cora' and 'BRS Carmem' – exhibited distinct profiles of UHPLC-MS features. In a study investigating the genetic bases of the untargeted metabolome of model plant species *Arabidopsis thaliana*, the authors demonstrated that recombinant inbred lines were chemically more diverse than the parents, highlighting the potential of classical breeding to induce chemical diversity.⁵⁴

Moreover, the results also demonstrated that large portions of the genome are responsible for controlling the chemical diversity, as shown for tomato in a later study.⁵⁵ In grapevine, the contents of berry anthocyanin, malic acid, and 6-carbon volatiles were shown to be determined by a set of genomic locations but influenced by other unrelated regions.⁴¹ In the current study, the integrative analyses of the phenolics, volatiles, and UHPLC-MS profiles reflected the genetic distance between the cultivars obtained from three generations of controlled crosses. The chemical profile of the juices also demonstrate metabolic changes unrelated to traits under selection during breeding, agreeing with the complex inheritance patterns of metabolites in plants.

CONCLUSIONS

The results of the current work demonstrate the correspondence between the genetic distance of grapevine cultivars and the chemical composition of the juices. Soluble sugar contents, and total anthocyanins and phenolics were less influenced by the environment, confirming their effectiveness as selective traits. Our findings also show that partial metabolic profiling of the juices, based on specific classes of compounds, as phenolics or volatiles, misrepresents the genetic relationships among the cultivars. Juices from the later generation of cultivars exhibit significant positive association with health-related phenolics and a more complex blend of volatiles, despite the absence of selection for these features. Future studies will address the influence of the genetic distance of the genotypes on the oenological properties of wines, since environmental adaptation and disease tolerance characteristics make the cultivars viable alternatives for more sustainable viticulture practices.

AUTHOR CONTRIBUTIONS

HAG Gomez: Methodology and investigation. GF Niederauer: Investigation. IO Minatel: Investigation. ERM Antunes: Data curation and analyses. MJ Carneiro: Methodology, investigation, and original writing, ACHF Sawaya: Data curation, supervision, and writing – reviewing and editing. MC Zanus: Supervision. V. Quecini: Conceptualization, data curation, and writing – reviewing and editing. PS Ritschel: Conceptualization, data curation, supervision, and writing – reviewing and editing, GPP Lima: Supervision and writing – reviewing and editing. MOM Marques: Data curation, supervision, and writing – reviewing and editing.

ACKNOWLEDGEMENTS

We would like to express our gratitude to Mr Roque Zillio at Embrapa for excellent management of the vineyards and assistance in berry harvesting. We also acknowledge the staff at Embrapa for carrying out the juice production.

FUNDING INFORMATION

The work was supported by a research grant Embrapa/SEG (20.18.01.019.00.00) to PS Ritschel. MOM Marques was the recipient of a productivity grant by the National Council for Scientific and Technological Development, CNPq (309 957/2015-0), HAG Gomez was supported by a Doctoral Students Abroad (PAEDEX/AUIP/PROPG) scholarship from São Paulo State University (UNESP), MJ Carneiro received a scholarship grant Embrapa/CNPq (404 250/2020-3), and GF Niederauer was supported by a PIBITI/CNPq/IAC scholarship (115240/2016-0).

CONFLICT OF INTEREST

The authors declare that they have no known competing financial interests or personal relationships that could have appeared to influence the work reported in this paper. The sponsors had no role in study design; in the collection, analysis and interpretation of data; in the writing of the report; or in the decision to submit the article for publication.

DATA AVAILABILITY STATEMENT

The data that support the findings of this study are available from the corresponding author upon reasonable request.

SUPPORTING INFORMATION

Supporting information may be found in the online version of this article.

REFERENCES

- Food and Agriculture Organization of the United Nations. FAOSTAT Statistical Database. [Online]. The United Nations, Food and Agriculture Organization, Rome (2023). Available: <https://www.fao.org/faostat/en/> [26 June 2023]
- Töpfer R and Trapp O, A cool climate perspective on grapevine breeding: climate change and sustainability are driving forces for changing varieties in a traditional market. *Theor Appl Genet* **135**:3947–3960 (2022). <https://doi.org/10.1007/s00122-022-04077-0>.
- Delrot S, Grimplet J, Carbonell-Bejerano P, Schwandner A, Bert P-F, Bavaresco L et al., Genetic and genomic approaches for adaptation of grapevine to climate change, in *Genomic Designing of Climate-Smart Fruit Crops*, ed. by Kole C. Springer, Cham, pp. 157–270 (2020). https://doi.org/10.1007/978-3-319-97946-5_7.
- Ritschel PS, Maia JDG, Protas JF d S, Guerra CC, Pereira GE and Lima M d S, The viticulture and agro-industry of American grape juice in a growing market. *Territoires du Vin [online]* **9** (2018). <https://preo.u-bourgogne.fr/territoiresduvin/index.php?id=1678>.
- Gomès É, Maillot P and Duchêne É, Molecular tools for adapting viticulture to climate change. *Front. Plant Sci* **12**:1–20 [online] (2021). <https://doi.org/10.3389/fpls.2021.633846>.
- Possamai T and Wiedemann-Merdinoglu S, Phenotyping for QTL identification: a case study of resistance to *Plasmopara viticola* and *Erysiphe necator* in grapevine. *Front. Plant Sci* **13**:1–22 [online] (2022). <https://doi.org/10.3389/fpls.2022.930954>.
- Zou C, Karn A, Reisch B, Nguyen A, Sun Y, Bao Y et al., Sun Q and Cadle-Davidson L haplotyping the *Vitis* collinear core genome with rhAmp-Seq improves marker transferability in a diverse genus. *Nature Comm* **11**:413 (2020). <https://doi.org/10.1038/s41467-019-14280-1>.
- Reshef N, Karn A, Manns DC, Mansfield AK, Cadle-Davidson L, Reisch B et al., Stable QTL for malate levels in ripe fruit and their transferability across *Vitis* species. *Hortic Res* **9**:uhac009 (2022). <https://doi.org/10.1093/hr/uhac009>.
- Zhu G, Gou J, Klee H and Huang S, Next-gen approaches to flavor-related metabolism. *Ann Rev Plant Biol* **70**:187–212 (2019). <https://doi.org/10.1146/annurev-arplant-050718-100353>.
- Zhu F, Wen W, Cheng Y, Alseekh S and Fernie AR, Integrating multiomics data accelerates elucidation of plant primary and secondary metabolic pathways. *Biotechnol* **4**:47–56 (2023). <https://doi.org/10.1007/s42994-022-00091-4>.
- Yang Y, Cuenca J, Wang N, Liang Z, Sun H, Gutierrez B et al., A key 'foxy' aroma gene is regulated by homology-induced promoter indels in the iconic juice grape 'Concord'. *Hortic Res* **7**:67 (2020). <https://doi.org/10.1038/s41438-020-0304-6>.
- Moreno-Olivares JD, Paladines-Quezada DF, Giménez-Bañón MJ, Bleda-Sánchez JA, Cebrián-Pérez A, Gómez-Martínez JC et al., Proanthocyanidins composition in new varieties descended from Monastrell. *J Sci Food Agric* **103**:5039–5049 (2023). <https://doi.org/10.1002/jsfa.12578>.
- Gardiman M, De Rosso M, De Marchi F and Flamini R, Metabolomic profiling of different clones of *Vitis vinifera* L. cv. "Glera" and "Glera lunga" grapes by high-resolution mass spectrometry. *Metabolomics* **19**:25 (2023). <https://doi.org/10.1007/s11306-023-01997-w>.
- This P, Jung A, Boccacci P, Borrego J, Botta R, Costantini L et al., Development of a standard set of microsatellite reference alleles for identification of grape cultivars. *Theor Appl Genet* **109**:1448–1458 (2004). <https://doi.org/10.1007/s00122-004-1760-3>.
- Araújo Jr AT, Bremm C, Longhi P, Maia JDG, Ritschel PS, Diversidade genética de cultivares para elaboração de suco de uva com o uso de marcadores moleculares SSR. In: ENCONTRO DE INICIAÇÃO CIENTÍFICA, 11.; ENCONTRO DE PÓS-GRADUANDOS DA EMBRAPA UVA E VINHO, 7., Resumos... Bento Gonçalves: Embrapa Uva e Vinho, 2013, p.42. Available: <https://www.alice.cnptia.embrapa.br/alice/bitstream/doc/979947/1/juniorResumosC2013.pdf> [15 April 2023]
- Jombart T, ADEGENET: a R package for the multivariate analysis of genetic markers. *Bioinformatics* **24**:1403–1405 (2008). <https://doi.org/10.1093/bioinformatics/btn129>.
- R Core Team, R: A language and environment for statistical computing, in *R Foundation for Statistical Computing*. Vienna, Austria (2021). Available: <https://www.R-project.org/> [11 March 2023].
- Lima MDS, Silani IDSV, Toaldo IM, Corrêa LC, Biasoto ACT, Pereira GE et al., Phenolic compounds, organic acids and antioxidant activity of grape juices produced from new Brazilian varieties planted in the northeast region of Brazil. *Food Chem* **161**:94–103 (2014). <https://doi.org/10.1016/j.foodchem.2014.03.109>.
- Organisation Internationale de la vigne et du vin (OIV), compendium of international methods of wine and must analysis, in *Organisation Internationale de la vigne et du vin*. Organisation Internationale de la vigne et du vin (OIV), Paris, France, (2021) Available: <https://www.oiv.int/public/medias/7907/oiv-vol1-compendium-of-international-methods-of-analysis.pdf>.
- MacGuire RG, Reporting of objective color measurements. *HortScience* **27**:1254–1255 (1992). <https://doi.org/10.21273/HORTSCI.27.12.1254>.
- Natividade MMP, Corrêa LC and Souza SVC d, Pereira GE and Lima LC de O, simultaneous analysis of 25 phenolic compounds in grape juice for HPLC: method validation and characterization of São Francisco Valley samples. *Microchem J* **110**:665–674 (2013). <https://doi.org/10.1016/j.microc.2013.08.010>.
- Giusti MM and Wrolstad RE, Characterization and measurement of anthocyanins by UV-visible spectroscopy. *Curr Protoc Food Anal Chem* **00**:F1.2.1–F1.2.13 (2001). <https://doi.org/10.1002/0471142913.faf0102s00>.
- da Silva JK, Cazarin CB, Correa LC, Batista AG, Furlan CP, Biasoto AC et al., Bioactive compounds of juices from two Brazilian grape cultivars. *J Sci Food Agric* **96**:1990–1996 (2016). <https://doi.org/10.1002/jsfa.7309>.
- Carmem BRS and Violeta BRS, Bonatto Machado de Castilhos M, Luiz Del Bianchi V, Gómez-Alonso S, García-Romero E and Hermosín-Gutiérrez I, sensory descriptive and comprehensive GC-MS as suitable tools to characterize the effects of alternative winemaking procedures on wine aroma. Part I. *Food Chem* **272**:462–470 (2019). <https://doi.org/10.1016/j.foodchem.2018.08.066>.
- Bonatto Machado de Castilhos M, Luiz Del Bianchi V, Gómez-Alonso S, García-Romero E and Hermosín-Gutiérrez I, Sensory descriptive and comprehensive GC-MS as suitable tools to characterize the effects of alternative winemaking procedures on wine aroma. Part II: BRS Rúbea and BRS Cora. *Food Chem* **311**:126025 (2020). <https://doi.org/10.1016/j.foodchem.2019.126025>.
- Van Den Dool H and Kratz DJ, A generalization of the retention index system including liner temperature programmed gas-liquid partition chromatography. *J Chromatogr* **11**:463–467 (1963).
- Adams RP, *Identification of Essential Oil Components by Gas Chromatography/Mass Spectrometry*, Vol. 4. Allured Publishing Corporation, Carol Stream (2007).
- Chambers M, MacLean B, Burke R, MacLean B, Burke R, Amode D et al., Tabb DL and Mallick PA cross-platform toolkit for mass spectrometry and proteomics. *Nature Biotech* **30**:918–920 (2012). <https://doi.org/10.1038/nbt.2377>.
- Smith CA, Want EJ, O'Maille G, Abagyan R and Siuzdak G, XCMS: processing mass spectrometry data for metabolite profiling using nonlinear peak alignment, matching and identification. *Anal Chem* **78**:779–787 (2006). <https://doi.org/10.1021/ac051437y>.
- Xia J and Wishart DS, Metabolomic data processing, analysis, and interpretation using MetaboAnalyst. *Curr Protoc Bioinformatics* **34**:14.10.1–14.10.48 (2011). <https://doi.org/10.1002/0471250953.bi1410s34>.
- Harrell F Jr, *Hmisc: Harrell Miscellaneous* [Online]. R package version 4.7–1 (2022). Available: <https://CRAN.R-project.org/package=Hmisc> [11 November 2022].

- 32 Wei T and Simko V, *R package 'corrplot': visualization of a correlation matrix* [Online]. R package version 0.92 (2022). Available: <https://github.com/taiyun/corrplot> [11 November 2022].
- 33 Lê S, Josse J and Husson F, FactoMineR: a package for multivariate analysis. *J Stat Softw* **25**:1–18 (2008). <https://doi.org/10.18637/jss.v025.i01>.
- 34 Kassambara A and Mundt F, *factoextra: Extract and Visualize the Results of Multivariate Data Analyses* [Online]. R package version 1.0.7 (2020). Available: <https://CRAN.R-project.org/package=factoextra> [11 November 2022].
- 35 Rohart F, Gautier B, Singh A and Lê Cao KA, mixOmics: an R package for omics feature selection and multiple data integration. *PLoS Comput Biol* **13**:e1005752 (2017). <https://doi.org/10.1371/journal.pcbi.1005752>.
- 36 Scrucca L, Fop M, Murphy TB and Raftery AE, mclust5: clustering, classification and density estimation using Gaussian finite mixture models. *R Journal* **8**:289–317 (2016).
- 37 Bougeard S and Dray S, Supervised multiblock analysis in R with the ade4 package. *J Stat Softw* **86**:1–17 (2018). <https://doi.org/10.18637/jss.v086.i01>.
- 38 Granato D, Carrapeiro M d M, Fogliano V and van Ruth SM, Effects of geographical origin, varietal and farming system on the chemical composition and functional properties of purple grape juices: a review. *Trends Food Sci Technol* **52**:31e48 (2016). <https://doi.org/10.1016/j.tifs.2016.03.013>.
- 39 Dal Santo S, Zenoni S, Sandri M, De Lorenzis G, Magris G, De Paoli E *et al.*, Tornielli GB and Pezzotti M grapevine field experiments reveal the contribution of genotype, the influence of environment and the effect of their interaction (G×E) on the berry transcriptome. *Plant J* **93**:1143–1159 (2018). <https://doi.org/10.1111/tpj.13834>.
- 40 Cramer GR, Cochetel N, Ghan R, Destrac-Irvine A and Delrot S, A sense of place: transcriptomics identifies environmental signatures in cabernet sauvignon berry skins in the late stages of ripening. *BMC Plant Biol* **20**:41 (2020). <https://doi.org/10.1186/s12870-020-2251-7>.
- 41 Alahakoon D, Fennell A, Helget Z, Bates T, Karn A, Manns D *et al.*, Berry anthocyanin, acid, and volatile trait analyses in a grapevine-interspecific F2 population using an integrated GBS and rhAmpSeq genetic map. *Plants (Basel)* **11**:696 (2022). <https://doi.org/10.3390/plants11050696>.
- 42 Garde-Cerdán T, González-Lázaro M, Marín-San Román S, Sáenz de Urturi I, Murillo-Peña R, Rubio-Bretón P *et al.*, Could foliar applications of methyl jasmonate and methyl jasmonate+urea improve must grape aroma composition? *J Sci Food Agric* **103**:4813–4825 (2023) Accepted Author Manuscript). <https://doi.org/10.1002/jsfa.12549>.
- 43 Dıblan S and Özkan M, Effects of various clarification treatments on anthocyanins, color, phenolics and antioxidant activity of red grape juice. *Food Chem* **352**:129321 (2021). <https://doi.org/10.1016/j.foodchem.2021.129321>.
- 44 Jurczyk M, Kasperczyk J, Wrześniok D, Beberok A and Jelonek K, Nanoparticles loaded with docetaxel and resveratrol as an advanced tool for cancer therapy. *Biomedicine* **10**:1187 (2022). <https://doi.org/10.3390/biomedicines10051187>.
- 45 Ng CX, Affendi MM, Chong PP and Lee SH, The potential of plant-derived extracts and compounds to augment anticancer effects of chemotherapeutic drugs. *Nutr Cancer* **74**:3058–3076 (2022). <https://doi.org/10.1080/01635581.2022.2069274>.
- 46 Pan Y, Li H, Zhang B, Deng Z and Shahidi F, Antioxidant interactions among hydrophilic and lipophilic dietary phytochemicals based on inhibition of low-density lipoprotein and DNA damage. *J Food Biochem* **46**:e14267 (2022). <https://doi.org/10.1111/jfbc.14267>.
- 47 Aubert C and Chalot G, Chemical composition, bioactive compounds, and volatiles of six table grape varieties (*Vitis vinifera* L.). *Food Chem* **240**:524–533 (2018). <https://doi.org/10.1016/j.foodchem.2017.07.152>.
- 48 Ji X-H, Wang B-L, Wang XD, Wang XL, Liu F-Z and Wang H-B, Differences of aroma development and metabolic pathway gene expression between Kyoho and 87-1 grapes. *J Integ Agric* **20**:1525–1539 (2021). [https://doi.org/10.1016/S2095-3119\(20\)63481-5](https://doi.org/10.1016/S2095-3119(20)63481-5).
- 49 Yao H, Jin X, Feng M, Xu G, Zhang P, Fang Y *et al.*, Evolution of volatile profile and aroma potential of table grape Hutaı-8 during berry ripening. *Food Res Intl* **143**:110330 (2021).
- 50 Ma Z, Yang S, Mao J, Yang S, Mao J, Li W *et al.*, Chen B effects of shading on the synthesis of volatile organic compounds in 'Marselan' grape berries (*Vitis vinifera* L.). *J Plant Growth Regul* **40**:679–693 (2021). <https://doi.org/10.1007/s00344-020-10123-2>.
- 51 Georgiadou EC, Mina M, Neoptolemos V, Koundouras S, D'Onofrio C, Bellincontro A *et al.*, The beneficial effect of leaf removal during fruit set on physiological, biochemical, and qualitative indices and volatile organic compound profile of the Cypriot reference cultivar 'Xynisteri'. *J Sci Food Agric* **103**:3776–3786 (2023). <https://doi.org/10.1002/jsfa.12268>.
- 52 Hall RD, D'Auria JC, Silva Ferreira AC, Gibon Y, Kruszka D, Mishra P *et al.*, High-throughput plant phenotyping: a role for metabolomics? *Trends Plant Sci* **27**:549–563 (2022). <https://doi.org/10.1016/j.tplants.2022.02.001>.
- 53 Ma A and Qi X, Mining plant metabolomes: methods, applications, and perspectives. *Plant Commun* **2**:100238 (2021). <https://doi.org/10.1016/j.xplc.2021.100238>.
- 54 Keurentjes JJ, Fu J, de Vos CH, Lommen A, Hall RD, Bino RJ *et al.*, The genetics of plant metabolism. *Nat Genet* **38**:842–849 (2006). <https://doi.org/10.1038/ng1815>.
- 55 Tieman D, Zhu G, Resende MF Jr, Lin T, Nguyen C, Bies D *et al.*, A chemical genetic roadmap to improved tomato flavor. *Science* **355**:391–394 (2017). <https://doi.org/10.1126/science.aal1556>.